FLEXIBLE EXPOSURE AND NODAL MESH TREATMENT IN THE 3D NODAL SIMULATOR MGRAC: APPLICATION TO A MTR CASE WITH AXIALLY MOVABLE ASSEMBLIES

Frederik Reitsma
NECSA
PO Box 582
Pretoria, 0001
South Africa
reitsma@aec.co.za

Erwin Müller
CompuSim AB
Strängnäsgatan 6
723 34, Västerås
Sweden
compusim@quicknet.se

ABSTRACT

The MGRAC code is a three-dimensional nodal simulator that has in recent years been applied extensively to research reactor, and in particular swimming-pool type materials testing reactor simulation. In the current production version of MGRAC the core nodal neutronic and the fuel exposure meshes are identical and the selected mesh is fixed for all fuel assemblies and for all cycle depletion calculations. This mesh assignment is considered a rather severe restriction since it makes it difficult to model fuel/reflector assemblies and irradiation rigs accurately.

This inflexibility in mesh assignment has been removed in the latest development version of MGRAC by allowing independent specification of the core nodal neutronic mesh and the exposure mesh for each individual fuel/reflector/rig assembly. Numerical results illustrating the impact of this change in mesh treatment with regard to cycle depletion calculations for an MTR core are presented. It is found that significant differences may be expected in cycle length and fissile material depletion for simulations performed with the new versus the old mesh treatments.

1. INTRODUCTION

Three-dimensional (3D) nodal simulators are widely used to model the steady-state neutronic and thermal-hydraulic behaviour of water-moderated nuclear reactors. The application of two-group nodal diffusion models to simulate the neutronic characteristics of power reactor cores is well established and forms the basis of many industrial 3D simulator codes. Employment of 3D nodal methods for research reactor simulation has as yet not reached the same level of maturity and has only in recent years become topical (see e.g. [1,2]). The MGRAC code [2] is one 3D nodal simulator that has an established position [3,4,5,6] in the area of swimming-pool type materials testing reactor (MTR) simulation. Originally, MGRAC was developed to cater for both MTR and pressurised-water reactor

(PWR) applications and as a consequence much of the technology relevant to power reactor simulation was adopted even for MTR simulation. In particular, a Cartesian geometry transverse-integration analytic nodal diffusion model with smoothly varying intra-nodal cross-sections was embraced as the neutronic solver and fuel depletion was modelled on a mesh structure completely consistent with the nodal neutronic mesh. The small size of an MTR core and the associated high neutron leakage demanded that at least one aspect of the traditional PWR nodal diffusion approach had to be abandoned, namely the use of only two neutron energy groups. The result was the development of a multi-group transverse-integration analytic nodal method [7] that allows for general up- and down-scattering of neutrons with no approximations whatsoever as regards the fission and scattering sources. In the nodal method the only approximation is that the transverse leakage and the intra-nodal spatially varying cross-sections are represented by low-order polynomials. The nodal coupling relations incorporate node-side flux discontinuity factors to represent cross-section homogenisation effects. Heterogeneous fluxes and powers are reconstructed by means of a modulation method employing multi-group flux and power form functions. The number of energy groups that can be handled is arbitrary and in routine MTR applications five or six groups have been found to be adequate [8].

After several years of experience with MGRAC as an MTR simulator, a need for enhancement of certain models was recognised. The two most important aspects that required improvement were the modelling of follower-type control rods that consist of a control rod section and a fuel follower section, and the fuel depletion-tracking model. This paper describes the latest developments in MGRAC to address the depletion tracking and follower-type control rod issues. Numerical results are presented to illuminate the consequences of the new developments.

2. APPROXIMATE FOLLOWER-TYPE CONTROL ROD MODELLING

The insertion and withdrawal of follower-type control rods has thus far been modelled in a highly approximate fashion in MGRAC by making use of the same mechanism that is employed for PWR control rods. This means that any control rod insertion is presumed to consist of the control rod being inserted into a stationary fuel assembly. In the case of a follower-type control rod this implies that the control rod section is assumed inserted into its associated fuel section (which in turn is assumed to be immobile and always present in the active core). The neutronic effect of control rod insertion is then modelled through appropriate modification of the fuel cross-sections (absorption as well as fission).

The application of the approximate control rod insertion model is illustrated in Figure 1 for three control bank positions. In each case the approximate modelling relative to the actual state of the control rod is shown as a pair of assemblies (the left member representing the approximate model). On the far left the situation when the control section of the control assembly is fully withdrawn (ARO) is depicted (the fuel follower section then physically covers the entire active height of the core). The opposite situation is shown to the far right with the control section totally inserted into the core (ARI) and the fuel follower section now protruding below the active core. In the centre the situation for a typical critical bank is shown. The approximate model does not truthfully reflect the actual physical situation.

Although the approximate control rod model may work quite well for a fresh control rod, it is clearly a dubious method as far as accuracy/realistic depletion tracking of the fuel follower section is concerned. With this approach, the fuel follower section is depleted continuously under conditions that are quite foreign to the actual (real) physical conditions when this section or part of it is withdrawn from the active core. Hence, this method will not only lead to a miss-prediction of the

reactivity worth of the fuel section but also of the fissile (U235) content of the fuel, the latter of which may have serious implications for fissile material inventory tracking. Accurate fissile material inventory tracking in MTRs is an issue of importance for both fuel economics and non-proliferation of nuclear materials (safeguard reports).

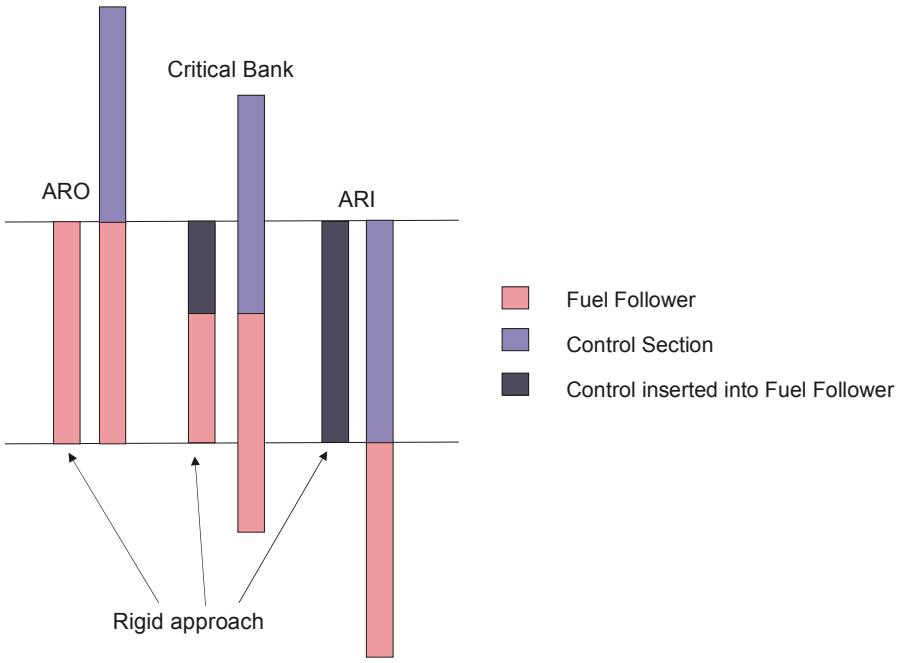

Figure 1. Approximate modelling relative to actual control rod status for a follower-type control rod.

Recognition of this and other problems posed by the axial motion of follower-type control rods, has lead to a revision of the MGRAC fuel depletion-tracking methodology with the objective of separating the core nodal neutronic and the fuel exposure meshes into semi-independent entities. Such a step facilitates realistic simulation of the depletion and axial motion of follower-type control rods and of axially movable fuel assemblies, irradiation rigs, etc.

3. FLEXIBLE EXPOSURE AND NODAL MESH TREATMENT

In the current production version of MGRAC the core nodal neutronic and fuel exposure meshes are identical and the selected mesh is fixed for all fuel assemblies and for all cycle depletion calculations. The axial nodal mesh structure must therefore be chosen carefully since it has to incorporate both the physical material layout of the various fuel/reflector/control assemblies and irradiation rigs and the nodal calculational mesh. This is practically impossible to accomplish since fuel assemblies, in-core reflector assemblies and irradiation rigs may each require totally different axial material meshes. Consequently, rather dubious approximations with regard to mesh assignment must be made to enable simulation of MTR cores with the current production version of MGRAC.

The above mentioned inflexibility in mesh assignment has been removed in the latest development version of MGRAC by allowing independent specification of the core nodal neutronic mesh and the exposure mesh for each individual fuel/reflector/control assembly and irradiation rig in the core. The nodal neutronic mesh that is used for the solution of the core nodal diffusion equations is quite

arbitrary and may be changed from fuel cycle to fuel cycle or even during a given fuel cycle. The exposure mesh for each individual assembly must, however, be chosen once and for all (per assembly) and must be chosen to be at least compatible with the axial material constitution of each assembly. Together, the mesh for depletion tracking and the axial material zones of an assembly define its exposure mesh. The new concept of exposure mesh is thus applicable even to the control rod sections of a follower-type control rod and to non-depletable reflector assemblies. The exposure mesh treatment also facilitates proper modelling of axial enrichment and burnable absorber zoning, if present (a feature that may be advantageously utilized in PWR and BWR applications).

The introduction of the independent exposure mesh is crucial for the explicit modelling of the axial motion of follower-type control rods. Since the exposure mesh does not have to coincide with the nodal neutronic mesh, it becomes a simple matter to accommodate axially mobile assemblies or control rods by simply adjusting the relative axial locations of the exposure meshes of these assemblies in the core model. However, to achieve this flexibility, a sophisticated axial homogenisation procedure must be employed to determine the cross-sections for the neutronic nodes. Such a procedure based on channel-wise one-dimensional (1D) diffusion calculations with explicit modelling of all axial heterogeneities imposed by exposure and neutronic meshes as well as by normal (non-follower-type) control rod insertions has been implemented in MGRAC. Depletion calculations require, in turn, an axial de-homogenisation procedure in order to extract the neutron fluxes for exposure meshes. This is achieved by carrying axial form factors representing the detailed heterogeneous fluxes from the 1D axial homogenisation calculations forward to the depletion calculations that are performed after the solution of the nodal diffusion problem for a given state point.

Depletion calculations encompass the updating of fuel exposures and isotopic number densities (of a number of important nuclides, mainly actinides) in each exposure mesh. Neutron fluxes are set to zero in all exposure meshes that lie outside the nodal neutronic domain (the spatial domain for which the nodal solution is sought). An exception is made for exposure meshes that lie only partly outside the neutronic domain. For them a linear extrapolation of the neutron fluxes is made to determine the average fluxes in these exposure nodes. It should be noted that the new flexible mesh approach does not in any way require that the neutronic domain be larger or different than that used with the old rigid mesh approach; this does not mean that enlargement of the neutronic domain to enhance physical accuracy is unnecessary.

4. THE TEST PROBLEM

The test problem used in the numerical studies of the new flexible mesh treatment is based on a typical core configuration of the SAFARI-1 reactor (a 20 MW tank-in-pool type materials testing reactor owned and operated by NECSA at its Pelindaba site near Pretoria, South Africa). The core layout used for the test is shown in Figure 2. The control assembly design and its representation in MGRAC are of particular interest in this work. For the benefit of readers not that familiar with MTR control assembly designs, Figure 3 illustrates the SAFARI-1 control assembly. It consists of an upper control section with cadmium box sandwiched between two aluminium boxes and a lower fuel follower section, which contains fifteen fuel plates. The two sections are joined together by an aluminium coupling piece. Although the coupling piece was ignored in the calculations performed in this work because the approximate mesh treatment cannot accommodate it, it can quite easily be taken into account with the new flexible mesh model.

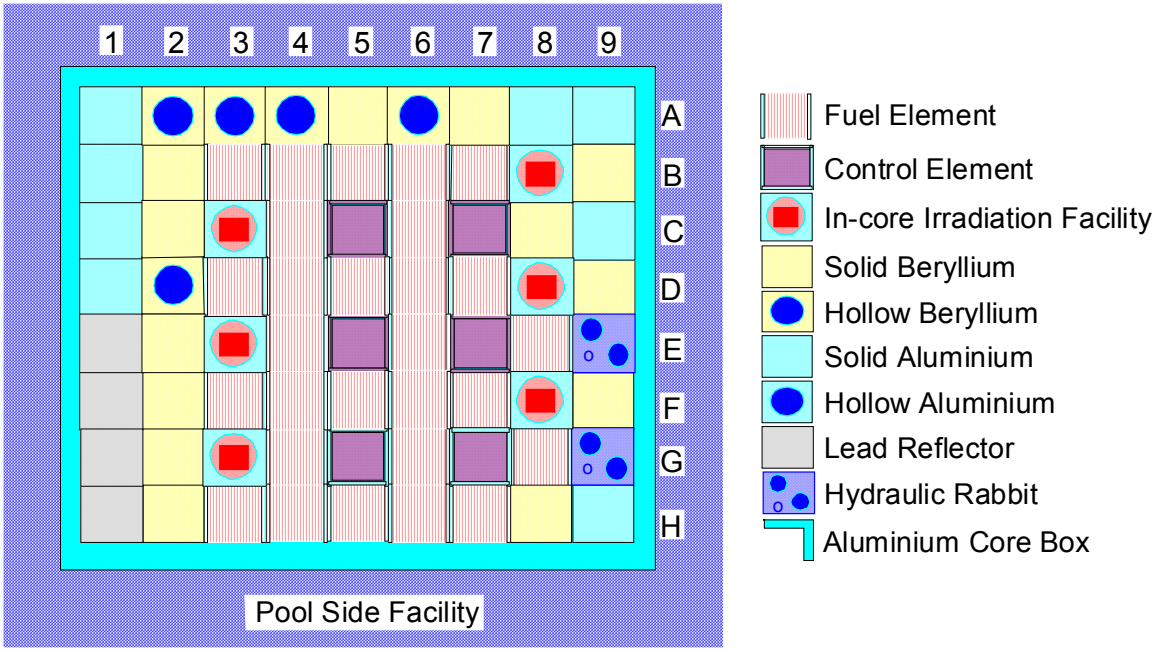

Figure 2. The test problem core layout.

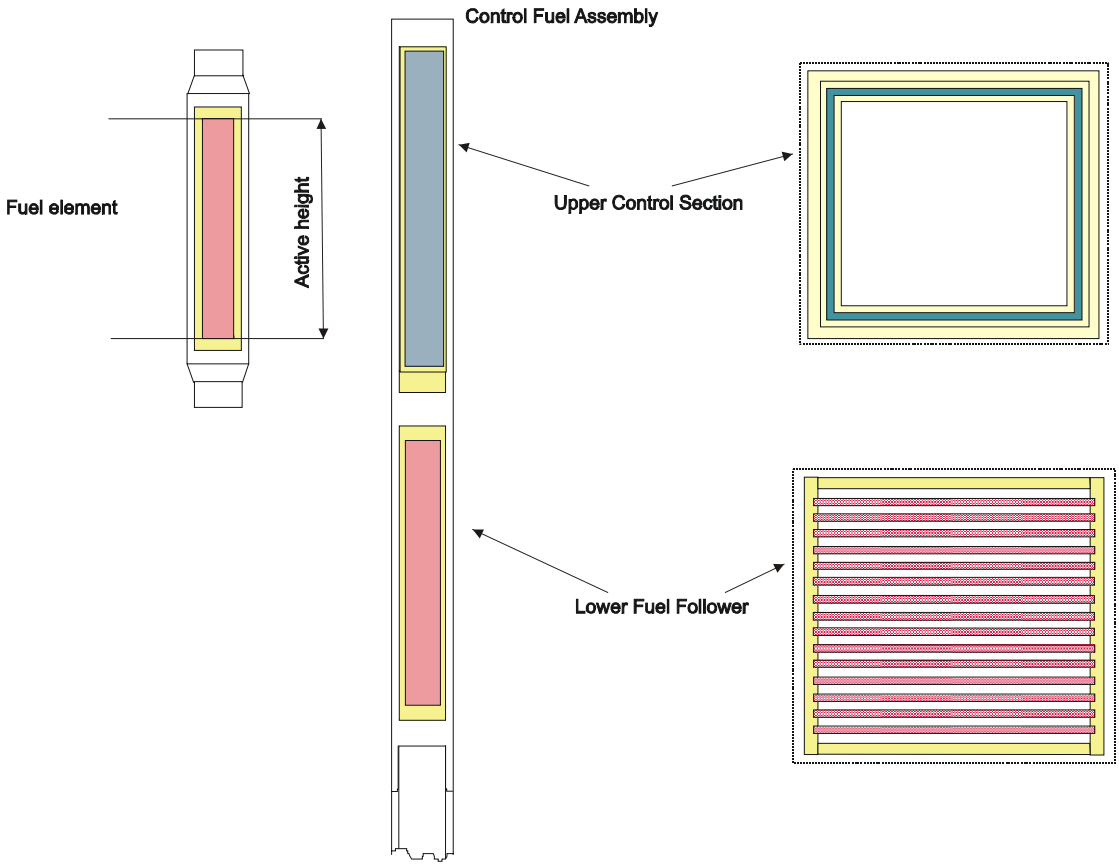

Figure 3. MTR control assembly with fuel follower.

5. NUMERICAL RESULTS

5.1 CYCLE CALCULATIONS

To demonstrate the utility of the flexible mesh treatment for follower-type control rod modelling, a series of depletion calculations for the test problem starting from exactly the same initial conditions were performed with the old and the new mesh treatments. Pre-determined fuel assembly exposures and isotopic number densities on a uniform exposure mesh that matches the neutronic mesh give the initial conditions for all cases. The control assembly fuel followers were, however, all assumed to be fresh and they were assigned exposure meshes similar to those of the normal fuel assemblies (i.e. exposures mesh sizes equal to the neutronic mesh sizes). Since the control sections are not burned, a single exposure mesh can be assigned to this part of each control rod. Differences in results would thus reflect only the impact of the control rod modelling (i.e. the explicit axial motion treatment versus the artificial insertion into the fuel follower section, and the control and fuel follower sections extending above and below the active core). Three calculation cases that are henceforth designated as Case A, Case B and Case C were considered.

In Case A the old rigid nodal mesh treatment was used to perform a single 18-day full-power cycle depletion calculation involving a critical control bank search at each depletion step (1-day depletion steps were used). The control bank consists of the six control rods all inserted to the same depth. The control rods were assumed inserted into the fuel follower section. In Case B the cycle depletion calculation was done with the new flexible mesh treatment and with the control rods and their fuel followers explicitly represented, but with the axial homogenisation model deactivated. This is consistent with Case A where volume weighting is used in partially rodded nodes. In Case C the same flexible mesh treatment as in Case B was used, but this time with axial homogenisation activated.

The neutronic core model consists of an active core (corresponding to the height of the active fuel region of the normal fuel assemblies) of height 59.37 cm covered by 6 neutronic nodes and bottom and top axial reflectors each of thickness 15 cm covered by 2 neutronic nodes each.

The critical bank insertions for this single cycle simulation (which is simply denoted as Cycle 1 since a further reload cycle is also simulated) are summarised in Table 1 below. This illustrates the type of differences that might be expected in actual MTR core follow simulations when the new control rod modelling approach is applied. The critical rod insertion fractions (in %) at various time points during the cycle are appreciably different for the three cases. For both Cases B and C the control bank needed to be inserted deeper into the core to achieve a critical state. Differences of up to 6.5% insertion depth (after 4 days burnup) were noticed between Cases A and C. This is equivalent to a 3.8 cm bank movement. The effect of the different mesh treatment alone (Case B compared to case A) is somewhat milder and varies between 1% and 3.8%. To place some perspective on these differences, it may be noted that every percentage difference in the control bank insertion depth at the beginning of cycle (BOC) can represent as much as 1 day of potential core operation. This is significant for an MTR for which a typical cycle length is of the order of 15 to 30 days. The impact of the axial homogenisation procedure during depletion is rather striking (as depicted by the last column in Table 1) and is clearly not to be neglected.

It should be noted that a significant part of the differences in critical bank insertions is due to the fact that the reactivity effects of those sections of the control rod that protrude outside the active core, but that fall within the domain of the axial reflectors, are accounted for in the flexible mesh model (cases B and C). In the old fixed mesh case (Case A) the axial reflectors contain neither control nor fuel material which means that the reactivity contributions of the said protruding sections are simply

ignored. The BOC difference between Case B and Case A illustrates this quite clearly since the only difference between these two cases at that point in time (where there is no depletion history difference) is the fact that Case B models the mentioned protruding sections. Case B thus includes both more control material and fuel material than Case A.

Table I. Control rod modelling effects for Cycle 1 (control bank % inserted)

	Case A	Case B	Case C	B – A	C – A	C – B
Case	Rigid mesh	New treatment Axhom=off	New treatment Axhom=on	Difference	Difference	Effect of Axhom
Critical bank						
BOC	46.5%	50.3%	50.6%	+3.8%	+4.1%	+0.3%
1d	41.9%	44.8%	47.8%	+2.9%	+5.9%	+3.0%
6d	37.4%	39.1%	43.7%	+1.7%	+6.3%	+4.6%
12d	34.2%	35.2%	37.8%	+1.0%	+3.6%	+2.6%
18d	25.5%	28.7%	31.3%	+3.2%	+5.8%	+2.6%
Relative CPU time	100.0	109.6	109.3	-	-	-

The CPU time differences quoted in Table 1 further show that the new method does not impose a significant additional computational burden (only about 10% increase in the total CPU time). Some of the additional time spent is due to different iteration behaviour and not only due to the time spent in performing the axial homogenization.

The different models also introduce meaningful differences in the assembly U-235 masses. The critical bank positions, the differences in the fuel follower axial burnup shapes (see Section 5.2) and the power delivered by the fuel followers below the active core all contribute to differences in the relative power distribution and therefore the mass distribution. Differences of between 1.2 and 1.8 grams in the U-235 content of individual control follower assemblies and up to 0.4 grams in individual fuel assembly masses were found after only one cycle. The U-235 mass differences (Case C – Case A) at the end of Cycle 1 are presented in Figure 4. Although the differences may seem small in comparison to the fresh U-235 content of 135 and 200 grams for control follower and fuel assemblies respectively, it is significant when compared to the cycle-average assembly U-235 burnup of about 13 grams.

1	2	3	4	5	6	7	8	9	
									A
		0.26	0.3	0.34	0.28	0.25			B
			0.36	-1.44	0.36	-1.18			C
		0.33	0.35	0.39	0.31	0.33			D
			0.37	-1.78	0.37	-1.53	0.26		E
		0.34	0.34	0.39	0.32	0.34			F
			0.35	-1.43	0.35	-1.25	0.24		G
		0.2	0.22	0.26	0.21	0.2			H

Figure 4. U-235 mass differences [gram] between cases A and C after Cycle 1.

In multi-cycle calculations the U-235 differences may impact significantly on the assembly masses and thus on fissile inventory reports where accuracy to 0.1 grams is normally required. Furthermore, in the case of control follower assemblies the contribution of the U-235 content to the reactivity worth of such assemblies may significantly affect subsequent predictions of start-up control bank insertion and cycle length. This in turn could lead to an unfavourable impact on core operations. In order to investigate the potential impact of the U-235 mass differences predicted by the two mesh models, a follow-up reload cycle case was simulated. A typical reload operation was executed with three feed (fresh) fuel assemblies introduced while the three most burned fuel assemblies were removed from the core. The fuel assemblies were reshuffled in a typical out-in loading pattern while the six burned control assemblies were left in the same positions.

This new cycle is simply denoted as Cycle 2 and also has a cycle length of 18 full-power days and a critical bank search is done at each 1-day burnup step in each calculation case (Cases A – C). In contrast to Cycle 1 the Cycle 2 starting exposures and axial burnup shapes in all fuel and control assemblies are different since they depend on the burnup history generated during Cycle 1, which will be different for each calculation case. The results for Cycle 2 are presented in Table II. While the maximum difference in the control bank insertion for Cycle 2 is found to be 6.5% as in the case of Cycle 1 it is not quite clear if larger differences would be found in multi-cycle calculations. The differences (Case C – Case A) in the end of cycle assembly U-235 masses are, on the other hand, significantly increased for Cycle 2 in comparison with those of Cycle 1: the maximum difference in the fuel follower assemblies has increased to 3.2 grams (from 1.8 grams) and to 0.7 gram (from 0.4 gram) in the normal fuel assemblies. This indicates, as might be expected, that the U-235 mass differences in the fuel follower sections are cumulative with time and could potentially lead to larger effects than those seen here. Since fuel and control assemblies typically reside in the core for up to nine cycles a complete history will have to be tracked to properly quantify the effect of the new flexible mesh approach, but this is left for further studies.

Table II. Control rod modelling effects for Cycle 2 (control bank % inserted)

	Case A	Case B	Case C	B – A	C – A	C – B
Case	Rigid mesh	New treatment Axhom=off	New treatment Axhom=on	Difference	Difference	Effect of Axhom
Critical bank						
BOC	36.6%	38.1%	42.7%	1.5%	6.1%	4.6%
1d	35.7%	37.0%	41.3%	1.3%	5.6%	4.3%
6d	32.4%	34.1%	35.4%	1.7%	3.0%	1.3%
12d	22.8%	25.1%	29.3%	2.3%	6.5%	4.2%
18d	18%	18.9%	18.8%	0.9%	0.8%	-0.1%

5.2 AXIAL BURNUP SHAPES

It is important to note that the axial burnup shape calculated in the control fuel follower differs significantly between the old and new approaches. Whereas the fuel follower exposure mesh coincided exactly with the nodal neutronic mesh in the old approach, the axial locations (relative to the neutronic meshes) of the exposure meshes vary in the new approach as a function of the control insertion depth. Hence, the new method allows for more realistic prediction of the axial exposure distribution within each fuel and control rod assembly. To illustrate this the axial burnup profiles of the fuel follower in position E5 at the end of Cycle 2 were compared for the three calculation cases.

This is presented in Figure 5. In the figure the burnup [MWd/t] achieved in the 6 axial exposure meshes (bottom to top) of the fuel follower is compared for the three calculation cases. It is immediately apparent that the burnup shape for the rigid mesh model is quite different than the shape resulting from the new mesh treatment. In Case B and Case C the upper section of the control fuel follower has the larger burnup. This is to be expected since the upper part of the fuel follower, positioned just below the control section, was positioned within the active core during the entire depletion history (control rods were never fully withdrawn during depletion). This behaviour is physically correct.

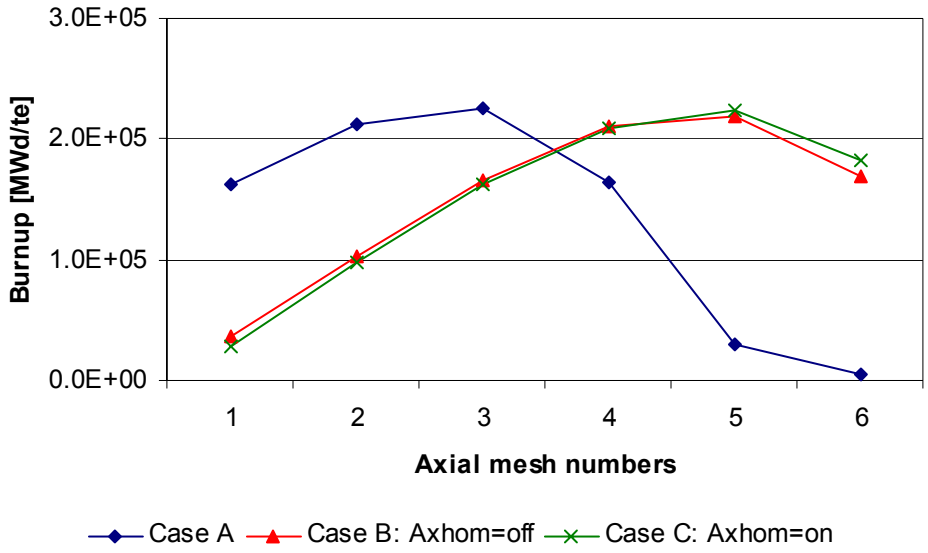

Figure 5. Axial burnup shape for control assembly E5 at end of Cycle 2.

In the rigid approach used in Case A, the lower section of the control fuel follower has depleted most while the upper part is much less depleted and even fresh in the uppermost axial mesh (number 6). This is not physically correct. From the representation in Figure 1 the reason for this axial burnup shape should be apparent. When the control assembly is inserted, the cross sections for the upper part of the (assumed) rigid fuel follower are corrected for rod insertions effects by adjustment of the absorption and fission cross sections. In particular, the fission cross sections are set to 0.0 in this rodded part. No fission and therefore no burnup in these meshes can therefore take place.

5.3 PRACTICAL CONSIDERATIONS

The question should also be asked as to how a user of the current production code should introduce the new flexible exposure and nodal mesh treatment in day to day core follow calculations. Since the exposure distributions produced by the old method are quite incorrect for the fuel follower assemblies, it may not be appropriate to start calculations with the new method by simply using the historical data generated by the old method. If this is done then larger than expected effects may be induced and critical control rod insertion depths may be severely miss-predicted. The usual remedy in such situations is to re-calculate a number of prior cycles using the new methodology so as to allow the adjustment of the burnup history to a level more consistent with the new method. To demonstrate the need for such an approach, the Cycle 1 calculation was repeated but this time not with fresh control

assembly fuel followers but with axial burnup shapes as pre-computed with the production code (old method). The results are shown in Table III.

Table III. Control rod modelling effects assuming "old method" fuel follower axial burnup shapes as the starting conditions (control bank % inserted)

	Case A	Case B	Case C	B – A	C – A	C – B
Case	Rigid mesh	New treatment Axhom=off	New treatment Axhom=on	Difference	Difference	Effect of Axhom
Critical bank						
BOC	36.6%	41.7%	46.6%	+5.1%	+10.0%	+4.9%
1d	35.5%	39.6%	44.9%	+4.1%	+9.4%	+5.3%
6d	31.7%	35.8%	39.6%	+4.1%	+7.9%	+3.8%
12d	22.3%	29.5%	32.0%	+7.2%	+9.7%	+2.5%
18d	17.6%	20.2%	25.3%	+2.6%	+7.7%	+5.1%

It is immediately clear that the differences between the cases are much larger than reported in Tables I and II. For example at BOC the critical control bank insertion depth of Case C is now some 10% larger than that of Case A, compared to a difference of only 4 % with the fresh fuel followers.

This example clearly shows that care has to be taken when the new improved flexible exposure and nodal mesh treatment is introduced in practical core follow calculations. The user will have to either correct the axial burnup shape or should go far back in the history and repeat the core follow calculations so that the "correct" burnup shape is gradually burned in for the fuel follower assemblies.

Other issues that are of practical interest are the axial size of the neutronic core (i.e. the sizes of the axial reflectors) and the sizes of the exposure meshes that should be used to achieve optimal results (accuracy versus computation cost). The larger the neutronic core, the better the reactivity effects of the sections of control rod that protrude outside the active core can be accommodated. The finer the exposure mesh, the more accurately the fuel depletion and especially the fissile material inventory can be tracked. Numerical studies of these aspects should be performed in order to establish an acceptable balance between accuracy and computational expense.

CONCLUSIONS

The flexible exposure and nodal mesh treatment that has been incorporated in the latest development version of the 3D nodal simulator MGRAC facilitates explicit modelling of follower-type control rods in MTRs. This offers the possibility of significantly reducing the uncertainty in computed control rod worth relative to the fixed-mesh scheme originally employed in MGRAC. Furthermore, it provides a means for improved fuel depletion-tracking and fissile material inventory reporting.

Numerical results for an MTR case demonstrate significant differences in control rod worths, fissile material inventories and control fuel follower axial burnup distributions between the new and old methodologies. While the new methodology is theoretically superior to the old one, comparison with experimental data is still required to establish the credibility of the new approach for MTR applications. Such comparisons are planned for the future.

The flexible exposure and nodal mesh treatment, while clearly applicable to MTR core calculations, is

also attractive for power reactor core analyses. A specific example where this approach is expected to be very fruitful is that of a BWR core with very heterogeneous (axially) fuel assemblies that have natural uranium blanket sections at assembly endpoints. Typically the blanket sections of different fuel assemblies have different heights with the consequence that the nodal mesh cannot be chosen to coincide with all blanket region boundaries. Nodes at or near assembly endpoints then contain a mixture (axially homogenised) of normal fuel and blanket materials. The fact that the actual exposures of the normal fuel and of the blanket materials in any given (axially homogenised) node are usually dramatically different poses a serious problem for any nodal method that employs a unified exposure and nodal neutronic mesh. Such a model does not provide for any means to extract realistic estimates of the exposures of the sub-nodes of any given node. The sub-node exposures are needed to interpolate in the cross-section tables and simply using node-average exposures may result in quite unrealistic values for sub-node cross-sections and pin-power form factors, especially in the blanket sub-nodes. A common consequence is that thermal load parameters such as LHGR (linear heat generation rate) may show unphysical spikes at the top or bottom of some fuel assemblies. With a flexible mesh treatment as described in this paper, this problem can be circumvented in an elegant way without the need for ad hoc approximations for sub-node exposures.

REFERENCES

1. F Reitsma and E. Z. Müller, " Evaluation of the Use of Nodal Methods for MTR Neutronic Analysis," (17^{th}) International Meeting on Reduced Enrichment for Research Reactors (RERTR), Williamsburg, Virginia, USA, September 18-23, 1994.
2. E. Z. Müller et. al., "Development of a Core Follow Calculational System for Research Reactors," 9th Pacific Basin Nuclear Conference, Sydney, Australia, May 1-6, 1994.
3. F. Reitsma and W. R. Joubert, "A Calculational System to Aid Economical Use of MTRs," International Conference on Research Reactor Fuel Management (RRFM '99), Bruges, Belgium, March 29-31, 1999.
4. G. Ball, "Efficient Use of Neutrons at SAFARI-1," International Conference on Research Reactor Fuel Management (RRFM '99), Bruges, Belgium, March 29-31, 1999.
5. P.F.A. de Leege, HP.M. Gibcus and F Reitsma, "HOR: Transition (HEU-LEU) Core Follow Comparisons between Different Computer Codes and Plant Data," M&C2001, Salt Lake City, Utah, USA, September 2001.
6. P.F.A. de Leege, HP.M. Gibcus and F Reitsma, "Reactivity Effects of a Research Reactor (HOR) during the Transition of a HEU to LEU Core," *PHYSOR 2002*, Seoul, Korea, 2002.
7. D. L. Vogel and Z. J. Weiss, "A General, Multigroup Formulation of the Analytic Nodal Method," International Topical Meeting on Advances in Reactor Physics, Charleston, South Carolina, USA, March 8-11, 1992.
8. W. R. Joubert, F. Reitsma and D. I. Tomasević, "Comparative Study of Nodal Cross Section Models applied to MTR Core Analysis," *PHYSOR 2002*, Seoul, Korea, 2002.